Comparative study of two different zeolites BEA and ZSM-5 exchanged by copper and iron via the oxidation of phenol by hydrogen peroxide

Fatiha Talhaoui[a], *Fatiha* Hamidi[b], *Fransisco* Medina[c]

[a] Mohamed Boudiaf University of Science and Technology, Faculty of Chemistry, Laboratory of Functional and Nanostructured Ecomaterials, Oran, Algeria.
e-mail: talhaoui.fatiha@live.com, **corresponding author**,
ORCID iD: https://orcid.org/0000-0001-8708-0717

[b] Mohamed Boudiaf University of Science and Technology, Faculty of Chemistry, Laboratory of Functional and Nanostructured Ecomaterials, Oran, Algeria.
e-mail: fatiha.hamidi@univ-usto.dz
ORCID iD: https://orcid.org/0009-0000-2216-8195

[c] Chemical Engineering Department, Rovira I Vigili University, Avda dels Països Catalans, 26, 43007, Tarragona, Spain
e-mail: francesc.medina@urv.cat
ORCID iD: https://orcid.org/0000-0002-3111-1542

https://doi.org/10.5937/vojtehg73-57849

FIELD: materials, chemical technology
ARTICLE TYPE: original scientific paper

Abstract:

Introduction/Purpose: Water pollution by organic compounds such as phenol poses a major environmental risk. This study aims to compare the catalytic efficiency of ZSM-5 and BEA zeolites, doped with iron (Fe) and copper (Cu), for the wet oxidation of phenol using hydrogen peroxide (H_2O_2).

Method: BEA and ZSM-5 zeolites were synthesized via hydrothermal methods, then ion-exchanged to incorporate Cu^{2+} and Fe^{2+}. The catalysts were characterized using XRD, FTIR, SEM, and XPS. Phenol oxidation was carried out at 80 °C in aqueous medium with an H_2O_2/phenol molar ratio ranging from 10:1 to 15:1. The reaction products were analyzed by HPLC.

Results: The crystalline structures of the zeolites were maintained after ion exchange. The metals were well dispersed on the surface. Fe-BEA and Fe-ZSM-5 catalysts showed the highest activity (up to 99% conversion), followed by Cu-BEA (88%) and Cu-ZSM-5 (68%). The pure zeolites exhibited low activity (<10%). The optimal H_2O_2/phenol ratio was 14:1. Fe-BEA proved to be the most effective, combining high activity with enhanced diffusion within the pores.

Conclusion: Iron-exchanged zeolites, particularly Fe-BEA, are highly effective catalysts for phenol oxidation in aqueous media, outperforming both copper-doped and pure forms. The porous structure and the nature of the metal are key factors determining catalytic performance.

*K*eywords: ZSM-5, B*EA, hydrogen peroxide, phenol oxidation, heterogeneous catalysis*

Introduction

Water pollution is a major threat to our health, to the environment and also to life, due to the strong industrialization which releases various toxic pollutants into the environment. Phenol is one of the most common forms of toxic chemical pollutants due to its frequency in waste water from various industries such as petrochemical (Alattar et al, 2024), pharmaceutical (Keshri & Dutt, 2021), stationery (Mohd, 2022), plastic (Shirvani et al, 2025), and agrifood (Said et al, 2021) .

Various technologies of treatments are used for the removal of phenol; the choice of treatment depends on the level of phenol concentration, ease of control, reliability and effectiveness of the treatment (Sun et al, 2025; Peng et al, 2023; Zhang et al, 2025; Liu et al, 2021; Khader et al, 2024).

Wet oxidation based on solid catalysts is one of the methods used for the treatment of organic effluents, when their concentrations are too low to be incinerated and too high for biological treatment (Mumtaz et al, 2024; Pan et al, 2025; Chen et al, 2025; Thomsen et al, 2022). Therefore, researchers have studied the catalytic activity of various types of catalysts in oxidation, which uses hydrogen peroxide under mild conditions (Broekman & Deuss, 2024; Cao et al, 2025).

Heterogeneous zeolite catalysts have high activity in oxidation reactions (Tian et al, 2024; Jiang et al, 2025). This efficiency depends considerably on the chemical composition, the method of preparation and the nature of metal species dispersed on the catalyst (Martins et al, 2022 ; Shaida et al, 2023; Toloza-Blanco et al, 2024; Dou, 2025).

Previous studies have reported that the oxidation of phenol by hydrogen peroxide on zeolite-based catalysts was influenced by several factors such as pH, temperature, nature of metallic species, and method of preparation (Jiang et al, 2017; Aziz et al, 2016; Liu et al, 2021; Saputera et al, 2021; Villegas et al, 2024).

The zeolites of types Y, BEA and ZSM-5 have wide industrial applications (Kumar et al, 2024; Ávila et al, 2024; Diallo et al, 2016; Zang et al, 2023; Wu et al, 2020; Liu et al, 2021; Lee et al, 2018; Liu et al, 2023).

These zeolites have particular and interesting catalytic properties, uniform microporous structure with a pore size perfectly calibrated (zeolites with large and medium pores), a large specific surface area, high acidity and high thermal stability.

Zeolites also have the property of great adaptability, while the sizes of these pores make zeolites potentially suitable for adsorption and conversion of large molecules with large applications in phenol oxidation reactions (Bania & Deka, 2013; Xie et al, 2017; Ghaffari et al, 2019; Nguyen & Carreon, 2022).

As far as the objective is concerned, the current study is the first of such research available in the open literature on the comparison between the two zeolites, BEA and ZSM-5, exchanged by copper and iron via the oxidation of phenols.

The main objective of this work is to carry out a comparative study between the catalytic performances of materials based on ZSM-5 and BEA zeolites doped with copper and iron prepared by cation exchange in phenol oxidation by hydrogen peroxide.

Experimental

Materials

The chemicals used in this research study are as follows: fumed silica (99%, Cab-oil), silica gel 60 (Merck), sodium aluminate (purchased from Reidel-Haën), tetraethylammonium hydroxide TEAOH (20%, Fluka), tetrapropylammonium bromide (TPA-Br, 99%, Merck), sodium hydroxide (NaOH; 98%), ammonium chloride (Sigma Aldrich), iron (II) chloride (Sigma Aldrich), copper (II) chloride (Sigma Aldrich), and phenol (Flucka, 99%). Throughout all experiments, demineralized water was used.

Synthesis of zeolites

Synthesis of BEA zeolites

A quantity of sodium-aluminate was added into an aqueous solution containing demineralized water and TEAOH under stirring at room temperature. The fumed silica was added delicately with vigorous stirring. The reaction mixture, containing a molar ratio of 2.07 Na_2O: 20 TEA_2O: Al_2O_3: 110 SiO_2: 1550 H_2O was subjected to stirring for 4 hours at room temperature.

The mixture was then crystallized in Teflon-lined stainless-steel autoclave at 150 °C for 3 days. The solid and liquid phases were separated

by centrifugation; the recovered solids were washed several times with distilled water, then dried at 80 °C and calcined at 550 °C for 8 hours.

Synthesis of ZSM-5

The ZSM-5 zeolite was synthesized from a solution of molar composition: $NaAlO_2$: 100 SiO_2: 12.5 Na_2O:25 TPABr 1100 H_2O. Tetrapropylammonium bromide is introduced in an alkaline solution of aluminate prepared in our laboratory from aluminum hydroxide. After obtaining a clear solution, the silica gel was added slowly in order to avoid the formation of lumps. The mixture formed was homogenized at room temperature under stirring for 4 hours before the hydrothermal treatment, then sealed in a stainless-steel autoclave. Hydrothermal crystallization was carried out at a temperature of 150 °C for two days. The solid recovered by filtration was washed several times with demineralized water, then dried overnight at 80 °C. Then, the product was calcined at 550°C for 8 hours.

Preparation of catalysts

Once the BEA and ZSM-5 zeolites were synthesized, and before copper and iron were incorporated, a first ion exchange step with ammonium chloride 0.01 mol was performed to replace the Na^+ cations present in the zeolite network by NH_4^+. Usually, this treatment is used to generate the acidic form of zeolites by thermal degradation of ammonium. The zeolite produced was subjected to calcination for 5 hours.

Chloride solutions were prepared by the introduction of copper chloride ($CuCl_2$) and iron chloride ($FeCl_2$) salts into closed glass reactors containing deionized water under agitation for a few minutes to complete the homogenization of solutions.

Then, the adequate amount of solid (HBEA or HZSM-5) was introduced in the reactor. The amount of solid was generally 1 g of solid in 100 cm^3 of 0.01 mol exchange solution. The ion exchange experiments were carried out at room temperature with stirring. The reaction time was set at 24 hours. The catalysts obtained are recovered by filtration, washing with demineralized water and drying overnight at 80 °C.

Characterizations

The solids prepared by ion exchange with copper and iron were characterized by X-ray diffraction (XRD) using a PHILIPS PW1710 diffractometer (copper tube lk. A: = 1.54060). The surface morphology of catalysts was examined using a scanning electron microscope (SEM) (FEG Quanta 200F FEI / Phillips). The Fourier transform infrared (FTIR)

spectroscopy analyses were carried out on a Nicolet FTIR 320 spectrophotometer in the range 4000 and 400 cm^{-1}. X-ray photoelectron spectroscopy (XPS) was performed using a Thermofisher ESCALAB 250 system with Al K-alpha radiation. The spectra acquired were analyzed by the XPS peak software.

Oxidation of phenol

The catalytic tests were carried out in a three-chamber flask, equipped with a water condenser, a thermometer and a magnetic stirrer. This bottle was placed in an oil bath and heated to 80°C under stirring at 500 rpm (Valkaj et al, 2011).

The reaction was carried out by dissolving 0.094 g of phenol in 100 cm^3 of water and transferred into a flask containing 0.01 g of catalyst. Once the reaction mixture had reached the desired temperature, hydrogen peroxide H_2O_2 (0.1 mol) was added dropwise into the reactor under stirring for 3 hours.

The samples taken during the reaction were filtered through 0.2 µm nylon membranes to analyze the reaction mixture. The concentration of phenol and its conversion products were analyzed by high performance liquid chromatography (HPLC).

Results and discussion

Characterization of catalyst

X-ray diffraction

The crystal structures of the prepared catalysts were verified by XRD analysis. Figure 1 represent the XRD spectra of the parent zeolites and their forms exchanged by the transition metals (iron and copper).

The comparison of these spectra revealed that all the distinctive lines of the BEA and ZSM-5 zeolites were observed after the cationic exchange, suggesting that the crystalline structure of both zeolites was preserved (Chen et al, 2024; Sazama et al, 2020; Gabrienko et al, 2025).

The BEA zeolite catalyst diffractograms shown in Figure 1 were characterized by a mixture of broad and subtle lines. This indicated the presence of a disordered structure formed by the intergrowth of two polytypes A and B as previously reported by Camblor et al. (1996).

All these catalysts revealed the same diffraction peaks that resemble those of the BEA zeolite at 7.8 ° and 22.5 (IZA International Zeolite Association, 2018). At the same time, the different lines of the zeolite catalysts ZSM-5 observed in Figure 1 exhibited the same peaks in the

range of 2θ = 7–9 ° and 23–25 ° which are corresponding to the standard phase of the ZSM-5 zeolite (Treacy & Higgins, 2007).

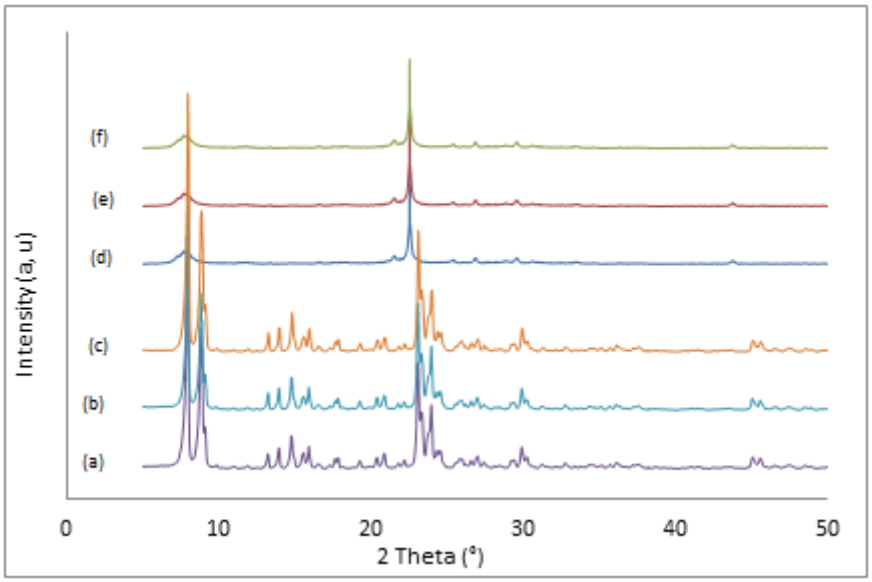

Figure 1- XRD patterns of ZSM-5 (a), Cu-ZSM-5 (b), Fe-ZSM-5 (c), BEA (d), Cu-BEA (e), and Fe-BEA (f) catalysts

In addition, no characteristic diffraction peak of copper and iron oxide (2θ approximately 35.5) was observed by XRD analysis in the modified samples (Ji et al, 2014; Sobuś et al, 2021), meaning that these two cations are entered into the interior of the zeolite, or they were highly dispersed on the surface of the zeolite (Song et al, 2016; Ren et al, 2019). Also, it can be suggested that the concentrations of Fe and Cu ions were below the XRD limits.

Thus, the intensities of each zeolite were reduced after the dispersion of metals Fe or Cu; this is due to the dispersion of iron or copper in ZSM-5 and BEA zeolites with X-rays absorption and the reduction of crystal degree of crystallinity (Sun et al, 2016).

Infrared spectroscopy

The fundamental vibration bands that characterize BEA and ZSM-5 zeolites lattice were observed in the range of 400-2000 cm^{-1}. The comparison of the BEA zeolite catalyst spectrum exchanged with copper and iron with those of zeolites synthesized (Figure 2) revealed the

presence of bands related to the characteristic vibrations of theBEA zeolite (Lin et al, 2020).

The absorption bands at 529-547 cm^{-1} and 433-434 cm^{-1} were due to the double cycles (D6R) and deformation of the internal bond Si -O in the SiO_4 tetrahedron.

The ratio of band intensities at 500 and 400 cm^{-1} was often used as an indicator of zeolite crystallinity (Coudurier et al, 1982). The samples exhibited a ratio ranged from 0.7 to 0.8 indicating the presence of high crystallinity materials. According to the literature (Bok et al, 1981, pp. 38505-38514), the ratio of bands was 0.8 for all BEA zeolites.

The bands at 1064-1076 cm^{-1} were due to the asymmetric elongation vibrations of internal links of TO_4 patterns. The vibration bands of symmetrical elongation at 628.76 cm^{-1} were attributed to the internal Si-O-Al bond, while the frequencies at 1226 cm^{-1} and 797-798 cm^{-1} were due to the bonds of the primary structural units.

The infrared spectra of ZSM-5 zeolites obtained before and after ion exchange with iron and copper shown in Figure 2 exhibited the characteristic bands of the ZSM-5 zeolite.

Therefore, the bands that appeared at 545.73-546.44 cm^{-1} were related to the vibrations of the secondary structural units (5-1) of an MFI zeolite.

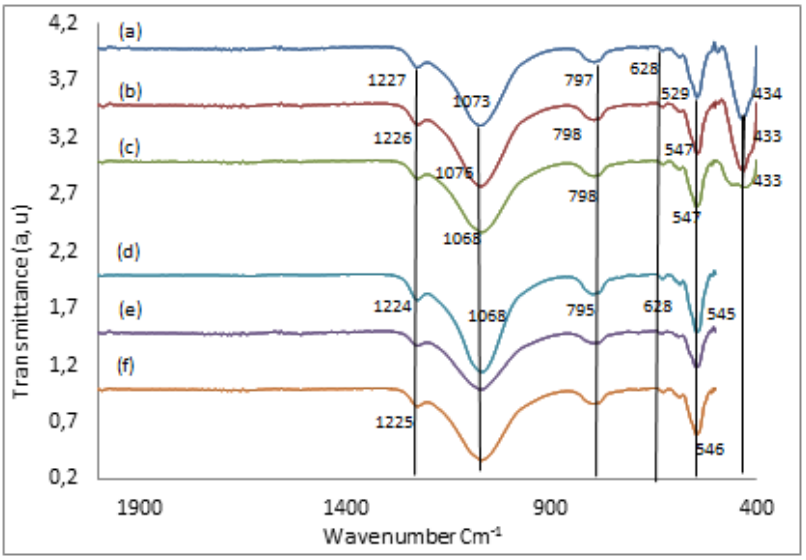

Figure 2- FTIR spectra of the samples: BEA (a), Fe-BEA (b), Cu-BEA (c), ZSM-5 (d), Fe-ZSM-5 (e), and Cu-ZSM-5 (f)

The asymmetric elongation vibration band at 1067.82-1068.86 cm^{-1} and the symmetrical elongation vibration band at 628.4-628.87 cm^{-1} were attributed to the internal bonds of Si-O-Al. The bands at the frequencies of 795.42-596.47 cm^{-1} and 1224.53-1225.10 cm^{-1} were due to the bonds of the primary structural units. The shifting of the bands was attributed to the exchange of hydrogen cations for cations of copper and iron.

Scanning electron microscope (SEM)

The morphology of the catalysts was examined using a scanning electron microscope (SEM). The images of different BEA and ZSM-5 catalysts are shown in Figure 3.

As reported, the crystal morphology of the iron and copper doped BEA zeolites revealed a large number of crystals with assemblages of very small crystals of the BEA zeolite.

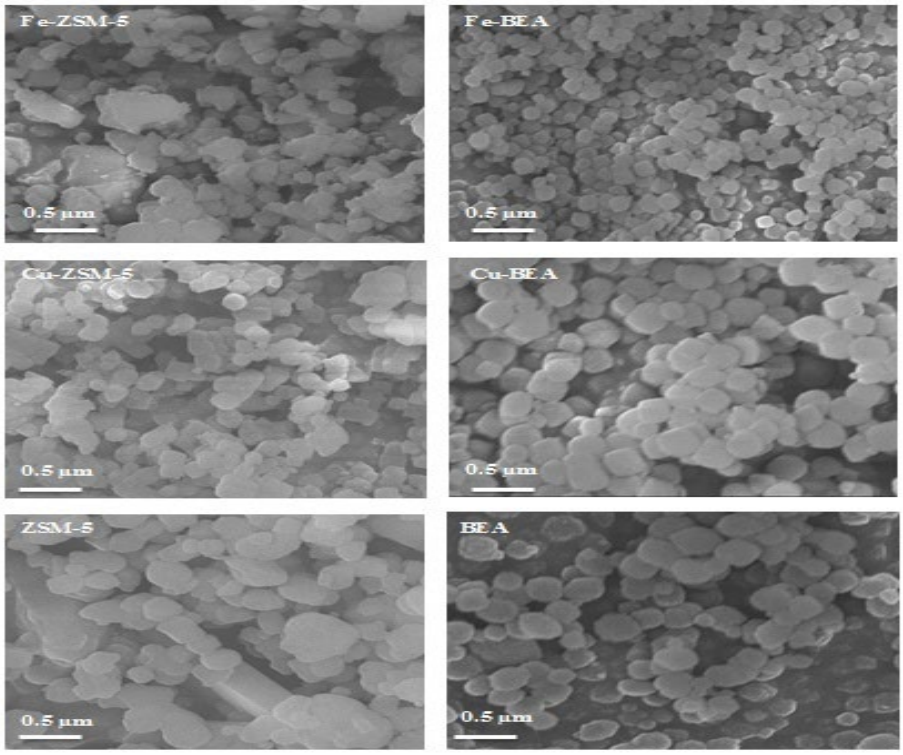

Figure 3- Scanning electron microscopy (SEM) images of BEA, Cu-BEA, Fe-BEA, ZSM-5, Cu-ZSM-5, and Fe-ZSM-5

The uniform shape and particle size were slightly greater than those of the parent zeolite. In fact, during the ion exchange process, the transition metals are distributed or doped on the parent zeolites.

Based on the images of different crystallite ZSM-5 zeolites, the images showed an agglomeration of small, medium-sized crystals of the order of 0.5 µm with a shape characteristic of the ZSM-5 zeolite. The particle size distribution and the morphology of the Cu-ZSM-5 and Fe-ZSM-5 catalysts are approximately the same as those of the parent ZSM-5 zeolite with no significant change in morphology. Furthermore, the modified products inherit the morphology of the parent zeolite after the ion exchange step.

X-ray photoelectron spectroscopy (XPS)

The chemical composition and the coordination between metal and M-zeolite (Fe or Cu) zeolite were identified by XPS analysis. The spectrums are depicted in Figure 4.

As shown in Figure 4.a, the spectra confirmed the presence of metal Fe in the modified zeolites, the presence of binding energy around 711.88-712 and 724.68-725.18 eV correspond to Fe 2p (3 / 2) and Fe 2p (1 / 2) (He et al, 2020), respectively, which are bound to Fe^{2+} ions (Lin et al, 2018).

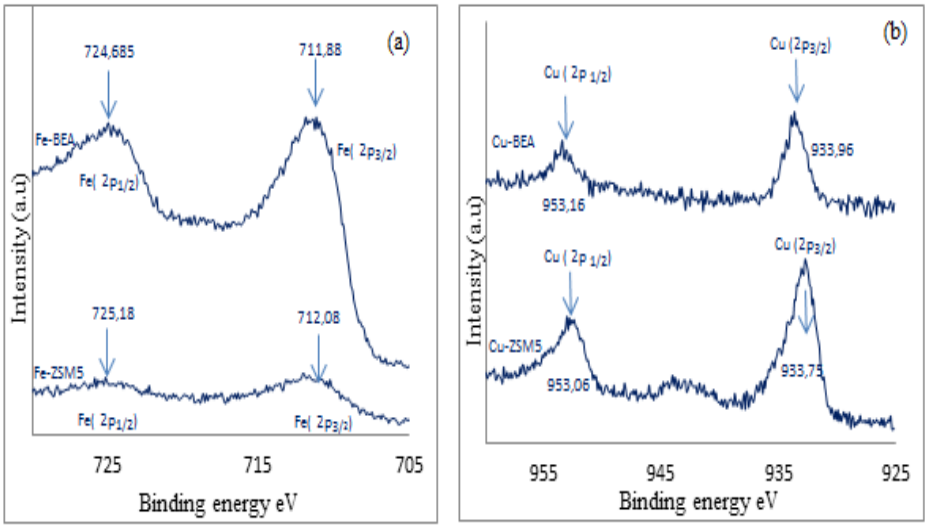

Figure 4 - X-ray photoelectron (XPS) spectra of modified zeolites (a) Fe 2p and (b) Cu 2p

The decrease in the peak intensities of Fe 2p indicated that the decline of iron species on the ZSM-5 zeolite surface might be due to ion

exchange causing the iron species found on the surface to become embedded inside the zeolite.

As shown in Figure 4.b, the XPS spectra of metal Cu confirmed its presence in the zeolites exchanged with narrow regions Cu 2p.

According to the literature (Wang et al, 2019), a binding energy of 932.5-952.3 eV corresponds to Cu 2p (3/2) and Cu 2p (1/2) attributed to Cu^{+} species, while peaks Cu 2p (3/2) and Cu 2p (1/2) located at 933.7 ± 0.2 eV and 953.7 ± 0.2 eV, were attributed to the Cu^{2+} species.

The Cu 2P (3/2) and Cu 2P (1/2) peaks shown in Figure 4.b and located at binding energies 933.7 ± 0.2 eV and 953.2 ± 0.2 eV are the essential characteristics of Cu^{2+} species.

Catalytic activity

Oxidant effect

A preliminary series of experiments was carried out to examine the behavior of zeolites containing iron, copper, and pure zeolites to distinguish the effect of adsorption and reaction.

Table 1- Conversion of phenol on zeolites: BEA, Cu-BEA, Fe-BEA, ZSM-5, Cu-ZSM-5, and Cu-ZSM-5) with and without oxidant (T = 80°C, Cc Ph= 0.01 mol/l, Cc H_2O_2 = 0.10 mol/l, mcat = 0.10 g/l, and pH = 4.2).

	Phenol + H_2O_2	ZSM5	ZSM5 + H_2O_2	Cu-ZSM5	Cu-ZSM-5 + H_2O_2	Fe-ZSM5	Fe-ZSM-5 + H_2O_2
X Ph %	35.7	6.36	29.38	9.69	68.03	6.16	98.1
	Phenol + H_2O_2	BEA	BEA + H_2O_2	Cu-BEA	Cu-BEA + H_2O_2	Fe-BEA	Fe-BEA + H_2O_2
X Ph %	35.7	6.98	30.31	8.45	88.61	7.33	99.3

At a temperature of 353 K under the conditions explained in the experimental section after 180 min of reaction, the results of these experiments are shown in Table 1.

During the evaluation of the prepared catalysts, a preliminary experiment showed that phenol can be oxidized by hydrogen peroxide in the absence of catalyst. The percentage of conversion was 35% after 3 h of reaction.

As shown in Table 1, the experiments performed with pure zeolites produced a conversion rate of 7% for the BEA zeolite and 6% for the ZSM-

5 zeolite in the absence of hydrogen peroxide as an oxidant. The results were quite similar to those of the zeolites doped with iron and copper with a slight difference between the pure BEA and ZSM-5 catalysts and the doped catalysts.

The results mentioned that the majority of removal phenol was carried out by adsorption while the percentage of removal by oxidation was almost negligible. Hence, the removal rate of phenol does not exceed 10%.

On the other hand, in the presence of H_2O_2, BEA and ZSM-5 catalysts exchanged with iron and copper are more active, with a conversion rate of 99% for Fe-BEA catalyst, 98% for Fe-ZSM-5 catalyst, 88% for the Cu-BEA catalyst, and 68% for the Cu-ZSM-5 catalyst.

This can be attributed to the limitation of diffusion of molecules into the pores.

Interestingly, phenol was removed more easily by the Fe-zeolite than that of Cu-zeolite catalysts, indicating the diffusion of phenol in the pores of the iron-doped zeolites rather than that of the doped zeolites of copper. This can be attributed to the thermodynamic properties and in particular to the electrochemical properties of iron compared to copper (Alejandre et al, 2000).

The molecular sizes of hydrogen peroxide and phenol are listed in Table 2 (Atoguchi et al, 2004).

The comparison between the data in Table 2 and the pore dimensions of the BEA and ZSM-5 zeolites mentioned that hydrogen peroxide and phenol can diffuse more easily in the pores of the BEA zeolite than that in the pores of the ZSM-5 zeolite.

Table 2 - Molecular size of phenol and hydrogen peroxide

Molecule	a, nm	b, nm	c, nm
Phenol	0.4792	0.4908	0.5090
H_2O_2	0.2476	0.2476	0.361

It can be suggested that zeolite catalysts containing iron and copper are active for the oxidation reaction of phenol by hydrogen peroxide.

Another suggestion is that the difference in catalyst activity is caused by the difference in the activity of zeolites. The redox properties of transition metal cations such as iron and copper species promoted the production of hydroxyl groups in the presence of hydrogen peroxide.

In addition, it is assumed that the zeolite acidity can influence the conversion of hydrogen peroxide, i.e., the highest rate of the formation of hydroxyl radicals is obtained with zeolites having a greater acidity (Bahranowski et al).

Effect of the molar ratio H_2O_2: phenol

The concentration of hydrogen peroxide plays an important role in the stability of a catalyst in the oxidation reaction. The final conversion values after 180 min of degradation of phenol at different molar ratios (H_2O_2: phenol) are given in Table 3.

Table 3 - Effect of the molar ratio H2O2: Phenol on the conversion of phenol on BEA and ZSM-5 catalysts exchanged with iron and copper at T = 80 ° C and pH = 4.2

	Conversion rate (%)		
	H_2O_2: Phenol 10 :1	H_2O_2: Phenol 14 :1	H_2O_2: Phenol 15 :1
Cu-ZSM-5	68,03	71,43	75,81
Cu-BEA	88,61	96,96	93,36
Fe-ZSM-5	98.1	99,01	99,09
Fe-BEA	99.3	99,7	99,54

As shown in Table 3, the oxidation of phenol was carried out using zeolite-based catalysts exchanged with iron and copper, employing three different H_2O_2: phenol molar ratios (10, 14, and 15). Increasing the H_2O_2: phenol molar ratio from 10:1 to 14:1 led to a significant improvement in the phenol conversion rate for all catalysts. This enhancement is attributed to the greater availability of hydrogen peroxide, which promotes the generation of hydroxyl radicals (HO•)—highly reactive species capable of effectively degrading phenol molecules. However, when the ratio reaches 15:1, a stagnation or slight decrease in performance is observed for certain catalysts (e.g., Cu-BEA). This phenomenon is explained by the formation of hydroperoxyl radicals (OOH•), which are less reactive than HO• and result from excess H_2O_2 (Equation 2). Subsequently, OH• radicals are

scavenged by OOH• and transformed into H_2O and O_2 according to Equation 3.

- Catalyst + $H_2O_2 \rightarrow$ OH• (1)
- OH• + $H_2O_2 \rightarrow$ OOH• + H_2O (2)
- OOH• + OH• $\rightarrow O_2 + H_2O$ (3)

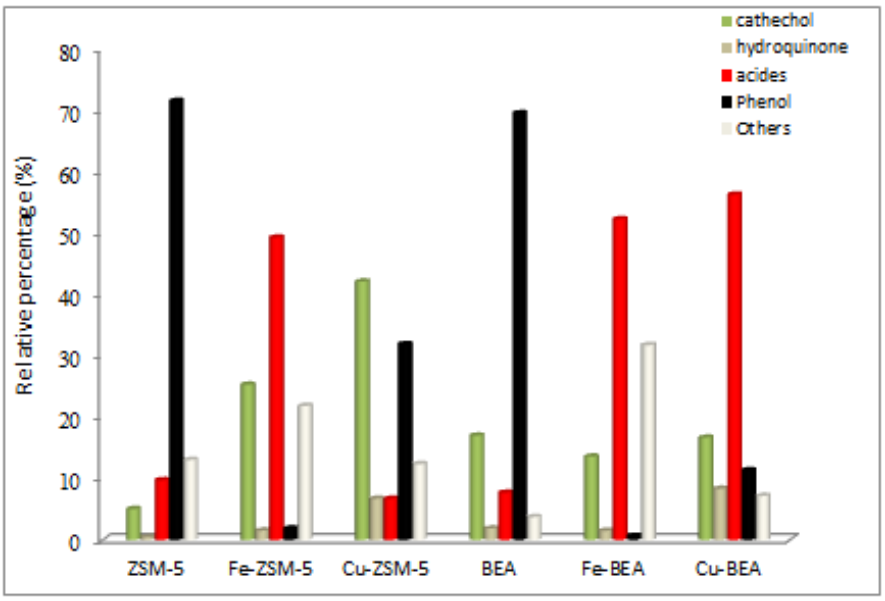

Figure 5-Distribution of by-products on catalysts based on M+/zeolites (T = 80°C, Cc Ph= 0.01 mol/l, Cc H_2O_2 = 0.10 mol/l, mcat = 0.10 g/l, and pH = 4.2)

The iron-doped catalysts (Fe-ZSM-5 and Fe-BEA) exhibit the highest conversion rates (up to 99.7%). This is due to the superior redox activity of iron for activating H_2O_2 and its strong ability to generate hydroxyl radicals. The BEA structure offers better diffusion than ZSM-5; however, even within the more restrictive ZSM-5 framework, iron remains highly active. The copper-doped catalysts (Cu-ZSM-5 and Cu-BEA) show lower performance compared to iron-based catalysts. Nonetheless, Cu-BEA outperforms Cu-ZSM-5, thanks to its more open porous structure that facilitates easier diffusion of reactants. However, copper is less efficient than iron in generating HO• species. It is well known that the catalytic oxidation of phenol in the liquid phase by hydrogen peroxide is a highly complex process, involving a series of parallel and consecutive reactions, with a wide range of intermediates and final products. These include aromatic compounds such as benzoquinone, hydroquinone, catechol,

carboxylic acids (acetic, maleic, oxalic, and fumaric acids), and other oxygenated compounds like aldehydes and ketones. At the beginning of the oxidation process, phenol can react with radicals generated from the decomposition of H_2O_2. The reaction medium initially turns dark brown due to the formation of by-products such as hydroquinone and catechol. Later, the solution becomes clear, indicating the formation of various acids and CO_2, as reported by Taran et al. (2018) and Devard et al. (2019)

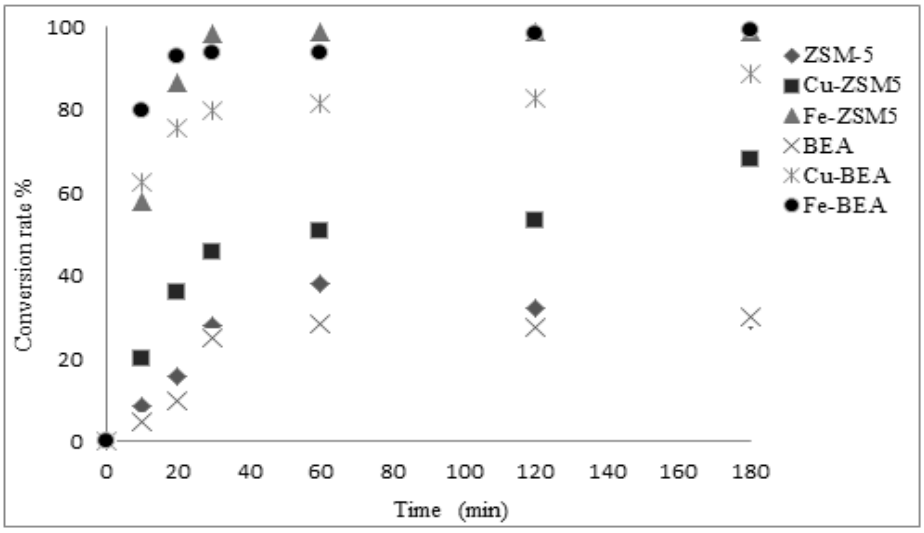

Figure 6 - Conversion of phenol as a function of time on pure catalysts and M + -zeolite catalysts (T = 80°C, CcPh= 0.01 mol/l, Cc H_2O_2 = 0.10 mol/l, mcat = 0.10 g/l, and pH = 4.2)

As depicted in Figure 6, the Fe-zeolite catalysts showed maximum activity with a conversion rate of 55% in the first 10 minutes and over 98% after 3 hours. The pure zeolite catalysts had a conversion rate of less than 10% during the first 10 minutes and it reached 30% after 3 hours.

On the other hand, the Cu-BEA catalyst showed an average catalytic efficiency with a rate of conversion of 62% in the first 10 minutes and 88% after 3 hours, while the Cu catalyst ZSM-5 showed minimal catalytic efficiency with a rate of conversion of 20% within the first 10 minutes and 68% after 3 hours.

Catalytic tests showed the catalytic activity of the Fe-BEA catalyst with a phenol conversion of 99%, which is very considerable compared to the other catalysts prepared.

The rapid decrease in the concentration of phenol can be explained by its adsorption on the catalyst. It is evident that zeolites doped with transit metals increased the conversion of phenol more than five times at the initial stage of the process.

According to this study, the BEA zeolite exhibited excellent results via the oxidation of phenol due to its structure with large pores and cavities resulting from the interconnection of its channels, the dimensions of pores being (6.4 - 7.6) Å2 along the axis [001] and (4.5 - 5.5 Å) along the axis [100]), at their high specific surface area (≥. 400 m^2 / g) (Selvam, 2003; Zhou et al, 2019), and its ion exchange capacity via transition metals.

Conclusion

The objective of this study was the wet oxidation of phenol with hydrogen peroxide on heterogeneous catalysts containing iron and copper under mild conditions.

The X-ray diffraction spectra indicated that the most of prepared zeolite catalysts exchanged with copper or iron exhibited diffraction peaks similar to those of pure zeolites. Then, the crystal structure was preserved during cation exchange for all catalysts based on exchanged zeolites.

Infrared, SEM, and XPS analyses confirmed the good dispersion of metals within the zeolite structure and the stability of the active phases on the catalyst surface. These characterizations also provided better insight into the interaction between the metals and the zeolitic support.

It can be concluded that all catalysts based on BEA and ZSM-5 zeolites doped with iron and copper are potentially active, in comparison with catalysts based on pure zeolites. They demonstrated high stability in aqueous media and are therefore suitable for use without causing metal pollution issues.

Regarding catalytic activity, phenol conversion rates reached approximately 70–90% for the ZSM-5 exchanged with copper and iron, while the doped BEA zeolites showed even higher conversions of 90–99%. In contrast, the pure zeolites exhibited significantly lower conversion rates, below 35%, thus confirming the beneficial effect of introducing transition metals, which are therefore favorable to be used without causing problems of metal pollution.

The efficiency of phenol oxidation strongly depends on two key factors:

- ✓ The H_2O_2: phenol ratio, a moderate excess of oxidant enhances conversion up to an optimal threshold.

- ✓ The nature of the metal cation, iron promotes the formation of oxidizing radicals more effectively than copper.

The most efficient combination is achieved with the Fe-BEA catalyst, which combines high catalytic activity with a porous structure that ensures optimal diffusion of reactants.

References

Alattar, S.A., Sukkar, K.A. & Alsaffar. M.A. 2024. Phenol removal from wastewater in petroleum refineries by managing flow characteristics and nanocatalyst in ozonized bubble column. *Journal of Petroleum Chemistry*, 159, pp.159-169. Available at: https://doi.org/10.1134/S0965544124020117

Alejandre, A., Medina, F., Rodriguez, X., Salagre, P. & Sueiras, J. E. 2000. Preparation and activity of copper, nickel and copper-nickel-al mixed oxides via hydrotalcite-like precursors for the oxidation of phenol aqueous solutions. *Journal of Studies in Surface Science and Catalysis*, 130, pp. 1763-1768. Available at: https://doi.org/10.1016/S0167-2991(00)80456-5

Atoguchi, T., Kanougi, T., Yamamoto, T. & Yao, S. 2004. Phenol oxidation into catechol and hydroquinone over H-MFI, H-MOR, H-USY and H-BEA in the presence of ketone. *Journal of Molecular Catalysis A: Chemical*, 220(2), pp.183-187. Available at: https://doi.org/10.1016/j.molcata.2003.10.026

Ávila, M.I., Alonso-Doncel, M.M., Briones, L., Gómez-Pozuelo, J., Escola, J.M., Serrano, D.P., Peral, A. & Botas, J.A. 2024. Catalytic upgrading of lignin-derived bio-oils over ion-exchanged H-ZSM-5 and H-beta zeolites. *Journal of Catalysis Today*, 427, p.114419. Available at : https://doi.org/10.1016/j.cattod.2023.114419

Aziz, A., Park, H., Kim, S. & Kim, K. S. 2016. Phenol and ammonium removal by using Fe-ZSM-5 synthesized by ammonium citrate iron source. *International Journal of Environmental Science and Technology*, 13, pp.2805–2816. Available at: https://doi.org/10.1007/s13762-016-1107-z

Bahranowski, K., Dula, R., Gasior, M., Łabanowska, M., Michalik, A., Vartikian, L. A. & Serwicka, E. M. 2001. Oxidation of aromatic hydrocarbons with hydrogen peroxide over Zn, Cu, Al-layered double hydroxides. *Journal of Applied clay science*, 18(1-2), pp.93-101. Available at: https://doi.org/10.1016/S0169-1317(00)00033-8

Bania, K. K. & Deka, R. C. 2013. Zeolite-y encapsulated metal picolinato complexes as catalyst for oxidation of phenol with hydrogen peroxide. *Journal of Physical Chemistry C*, 117(22), pp.11663-11678. Available at: https://doi.org/10.1021/jp402439x

Bok, T. O., Andriako, E. P., Knyazeva, E. E. & Ivanova, I.I. 2020. Engineering of zeolite BEA crystal size and morphology via seed-directed steam assisted conversion. *Journal of Rsc Advances* , 10 (63), 38505-38514. Available at: https://doi.org/10.1039/D0RA07610D

Broekman, J. O. P. & Deuss, P. J. 2024. Insights into the benign, selective catalytic oxidation of HMF to HMFCA in water using $[Mn^{IV}_2 (\mu\text{-}O)_3 (tmtacn)_2]^{2+}$ and Hydrogen Peroxide. *Journal of Organometallics*, *43*(11), pp.1264-1275. Available at: https://doi.org/10.1021/acs.organomet.4c00109

Camblor, M.A., Corma, A. & Valencia, S. 1996. Spontaneous nucleation and growth of pure silica zeolite-β free of connectivity defects. *Journal of Chemical Communications*, 20, pp.2365-2366. Available at: https://doi.org/10.1039/CC9960002365

Cao, K., Yang, F., Wan, H., Duan, X., Shi, J. & Sun, Z. 2025. A selective oxidative depolymerization of larch lignin to ethyl vanillate by multifunctional catalysts combining alkaline ionic liquid and polyoxometalates with hydrogen peroxide. *International Journal of Biological Macromolecules*, 295, p.139642. Available at: https://doi.org/10.1016/j.ijbiomac.2025.139642

Coudurier, G., Naccache, C. & Vedrine, J.C. 1982. Uses of IR spectroscopy in identifying ZSM zeolite structure. *Journal of the Chemical Society, Chemical Communications*, 24, pp.1413–1415. Available at: https://doi.org/10.1039/C39820001413

Chen, X., Zhou, S., Wang, L., Zhang, C., Gao, S., Yu, D., Cheng, Y., Xiaoqiang, V., Yu, X. & Zhao, Z. 2024. Facile preparation of Fe-Beta zeolite-supported transition metal oxide catalysts and their catalytic performance for the simultaneous removal of NOx and soot. *Chinese Journal of Chemical Engineering*, 76, pp.10-20. Available at: https://doi.org/10.1016/j.cjche.2024.07.016

Chen, Z., Meng, G., Han, Z., Li, H., Chi, S., Hu, G. & Zhao, X. 2025. Interfacial anchoring cobalt species mediated advanced oxidation: Degradation performance and mechanism of organic pollutants. *Journal of Colloid and Interface Science*, *679*, pp.67-78. Available at: https://doi.org/10.1016/j.jcis.2024.10.097

Devard, A., Brussino, P., Marchesini, F. A. & Ulla, M. A. 2019. Cu (5%)/Al_2O_3 catalytic performance on the phenol wet oxidation with H_2O_2: Influence of the calcination temperature. *Journal of Environmental Chemical Engineering*, 7(4), p.103201. Available at: https://doi.org/10.1016/j.jece.2019.103201

Diallo, M. M., Mijoin, J., Laforge, S. & Pouilloux, Y. 2016. Preparation of Fe-BEA zeolites by isomorphous substitution for oxidehydration of glycerol to acrylic acid. *Journal of Catalysis Communications*, 79, pp. 58-62. Available at: https://doi.org/10.1016/j.catcom.2016.03.003

Dou, X., Yan, T., Li, W., Zhu, C., Chen, T., Lo, B. T. W., Xiao,H. & Liu, L. 2025. Structure–reactivity relationship of zeolite-confined Rh catalysts for hydroformylation of linear α-olefins. *Journal of the American Chemical Society*, 147 (3), pp. 2726–2736. Available at: https://doi.org/10.1021/jacs.4c15445

Gabrienko, A. A., Kolganov, A. A., Yashnik, S. A., Kriventsov, V. V. & Stepanov, A. G. 2025. Methane to methanol transformation on Cu^{2+}/H-ZSM-5 zeolite. characterization of copper state and mechanism of the reaction. *Chemistry–A European Journal*, 31(10), e202403167. Available at: https://doi.org/10.1002/chem.202403167

Ghaffari, Y., Gupta, N. K., Bae, J. & Kim, K. S. 2019. Heterogeneous catalytic performance and stability of iron-loaded ZSM-5, zeolite-A, and silica for phenol

degradation: a microscopic and spectroscopic approach. *Journal of Catalysts*, *9*(10), p.859. Available at: https://doi.org/10.3390/catal9100859

He, Y., Lin, H., Luo, M., Liu, J., Dong, Y. & Li, B. 2020. Highly efficient remediation of groundwater co-contaminated with Cr (VI) and nitrate by using nano-Fe/Pd bimetal-loaded zeolite: process product and interaction mechanism. *Journal of Environmental Pollution*, 263, p.114479. Available at: https://doi.org/10.1016/j.envpol.2020.114479

Hunt, J.P. & Taube, H. 1952. The photochemical decomposition of hydrogen peroxide. *Journal of the American Chemical Society*, 74(23), pp.5999–6002. Available at: https://doi.org/10.1021/ja01143a052

IZA International Zeolite Association. 2018. *Database of Zeolite Structures*. [online] Available at: https://www.iza-structure.org/databases/ [Accessed : le 27 April 2025]

Ji, F., Li, C., Liu, Y. & Liu, P. 2014. Heterogeneous activation of peroxymonosulfate by Cu/ZSM5 for decolorization of Rhodamine B. *Journal of Separation and Purification Technology* , 135 , pp.1-6. Available at: https://doi.org/10.1016/j.seppur.2014.07.050

Jiang, S., Zhang, H., Yan, Y. & Zhang, X. 2017. Preparation and characterization of porous Fe-Cu mixed oxides modified ZSM-5 coating/PSSF for continuous degradation of phenol wastewater. *Journal of Microporous and Mesoporous Materials*, 240, pp.108-116. Available at : https://doi.org/10.1016/j.micromeso.2016.11.020

Jiang, Y., Yu, T., Zeng, S. & Luo, W. 2025. Direct and selective oxidation of methane into methanol over Cu/Fe-containing zeolites. *Journal of Molecular Catalysis*, 571, p.114721. Available at: https://doi.org/10.1016/j.mcat.2024.114721

Keshri, V. & Dutt, KR. 2021. Inhibitory effect of phenolic and flavonoidal content of H. indicum root extract on 1,1-diphenyl-2-picrylhydrazyl radicals. *Research Journal of Pharmaceutical and Technology*, 14(1), pp.235-238. Available at: 10.5958/0974-360X.2021.00041.X

Khader, E. H., Khudhur, R. H., Mohammed, T. J., Mahdy, O. S., Sabri, A. A., Mahmood, A. S. & Albayari, T. M. 2024. Evaluation of adsorption treatment method for removal of phenol and acetone from industrial wastewater. *Journal of Desalination and Water Treatment*, 317, p.100091. Available at: https://doi.org/10.1016/j.dwt.2024.100091

Kumar, N. D. & Swaminathan, M. 2024. Review on hierarchically porous BEA and ZSM-5 zeolites and Its industrial catalytic applications. *Journal of ES Materials & Manufacturing*, 24, p.1151. Available at: https://doi.org/10.30919/esmm1151

Lee, K. X., Tsilomelekis, G. & Valla, J. A. 2018. Removal of benzothiophene and dibenzothiophene from hydrocarbon fuels using CuCe mesoporous Y zeolites in the presence of aromatics. *Journal of Applied Catalysis B: Environmental*, 234, pp.130-142. Available at: https://doi.org/10.1016/j.apcatb.2018.04.022

Lin, Q., Feng, X., Zhang, H., Lin, C., Liu, S., Xu, H. & Chen, Y. 2018. Hydrothermal deactivation over CuFe/BEA for NH3-SCR. *Journal of industrial and engineering chemistry*, 65, pp.40-50. Available at: https://doi.org/10.1016/j.jiec.2018.04.009

Lin, Q., Liu, S., Xu, S., Liu, J., Xu, H., Chen, Y. & Dan, Y. 2020. Fabricate surface structure-stabilized Cu/BEA with hydrothermal-resistant via si-deposition for NOx abatement. *Journal of Molecular Catalysis*, 495, p.111153. Available at: https://doi.org/10.1016/j.mcat.2020.111153

Liu, H., Kim, G. E., Hong, C. O., Song, Y. C., Lee, W. K., Liu, D., Jang, S.H. & Park, Y. K. 2021. Treatment of phenol wastewater using nitrogen-doped magnetic mesoporous hollow carbon. *Journal of Chemiosphere*, 271, p.129595. Available at: https://doi.org/10.1016/j.chemosphere.2021.129595

Liu, T., Wang, H., Hu, Z. & Wei, F. 2021. Highly efficient adsorption of thiol compounds by ZSM-5 zeolites: Governing mechanisms. *Journal of Microporous and Mesoporous Materials*, *316*, p.110968. Available at: https://doi.org/10.1016/j.micromeso.2021.110968

Liu, Y., Lu, H. & Wang, G. 2021. Preparation of CuO/HZSM-5 catalyst based on fly ash and its catalytic wet air oxidation of phenol, quinoline and indole. *Journal of Materials Research Express*, 8(1), p.015503. Available at: https://doi.org/10.1088/2053-1591/abd6a4

Liu, Y., Osta, E. H., Poryvaev, A. S., Fedin, M. V., Longo, A., Nefedov, A. & Kosinov, N. 2023. Direct conversion of methane to zeolite-templated carbons, light hydrocarbons, and hydrogen. *Journal of Carbon*, 201, pp.535-541. Available at: https://doi.org/10.1016/j.carbon.2022.09.050

Martins, A., Nunes, N., Carvalho, A. P. & Martins, L. M. 2022. Zeolites and related materials as catalyst supports hydrocarbon oxidation reactions. *Journal of Catalysts*, 12 (2), p.154. Available at: https://doi.org/10.3390/catal12020154

Mohd, A. 2022. Presence of phenol in wastewater effluent and its removal: an overview. *International Journal of Environmental Analytical Chemistry*, 102(6), pp.1362-1384. Available at: https://doi.org/10.1080/03067319.2020.1738412

Mumtaz, H., Werle, S. & Sobek, S. 2024. A waste wet oxidation technique as a solution for chemical production and resource recovery in Poland. *Journal of Clean Technologies and Environmental Policy*, 26(5), pp.1363-1382. Available at: https://doi.org/10.1007/s10098-023-02520-4

Nguyen, H. M. & Carreon, M. L. 2022. Non-thermal plasma-assisted deconstruction of high-density polyethylene to hydrogen and light hydrocarbons over hollow ZSM-5 microspheres. *Journal of ACS Sustainable Chemistry & Engineering*, 10(29), pp. 9480-9491.

Available at: https://doi.org/10.1021/acssuschemeng.2c01959

Pan, C., Zhang, Q., Zhang, W., Bao, J., Dai, G., Liu, S.& Lan, J. 2025. Wet scrubbing coupled with advanced oxidation process for removal of chlorobenzene: A study of performance and mechanisms. *Journal of Environmental Research*, 268, p.120779.

Available at: https://doi.org/10.1016/j.envres.2025.120779

Peng, J., Zhou, P., Zhou, H., Huang, B., Sun, M., He, CS., Zhang, H., Ao, Z., Liu, W. & Lai, B. 2023. Removal of phenols by highly active periodate on carbon nanotubes: A mechanistic investigation. *Journal of Environmental Science & Technology*, 57(29), pp.10804–10815.

Available at: https://doi.org/10.1021/acs.est.2c08266

Ren, T. I. A. N., WANG, S. Y., LIAN, C. S., Xu, W. U., Xia, A. N. & XIE, X. M. 2019. Synthesis of the hierarchical Fe-substituted porous HBeta zeolite and the exploration of its catalytic performance. *Journal of Fuel Chemistry and Technology*, 47(12), pp.1476-1485. Available at: https://doi.org/10.1016/S1872-5813(19)30059-3

Said, K. A. M., Ismail, A. F., Karim, Z. A., Abdullah, M. S. & Hafeez, A. 2021. A review of technologies for the phenolic compounds recovery and phenol removal from wastewater. *Process Safety and Environmental Protection*, *151*, pp. 257-289. Available at: https://doi.org/10.1016/j.psep.2021.05.015

Saputera, W. H., Putrie, A. S., Esmailpour, A. A., Sasongko, D., Suendo, V. & Mukti, R. R. 2021. Technology advances in phenol removals: Current progress and future perspectives. *Journal of Catalysts*, 11(8), p.998. Available at: https://doi.org/10.3390/catal11080998

Sazama, P., Moravkova, J., Sklenak, S., Vondrova, A., Tabor, E., Sadovska, G. & Pilar, R. 2020. Effect of the nuclearity and coordination of Cu and Fe sites in β zeolites on the oxidation of hydrocarbons. *Journal of ACS Catalysis*, 10(7), pp.3984-4002. Available at: https://doi.org/10.1021/acscatal.9b05431

Selvam, T., Bandarapu, B., Mabande, G. T. P., Toufar, H. & Schwieger, W. 2003. Hydrothermal transformation of a layered sodium silicate, kanemite, into zeolite Beta (BEA). *Journal of Microporous and Mesoporous Materials*, 64(1-3), 41-50. Available at: https://doi.org/10.1016/S1387-1811(03)00508-0

Shaida, M. A., Verma, S., Talukdar, S., Kumar, N., Mahtab, M. S., Naushad, M. & Farooqi, I. H. 2023. Critical analysis of the role of various iron-based heterogeneous catalysts for advanced oxidation processes: A state of the art review. *Journal of Molecular Liquids*, 374, p.121259. Available at: https://doi.org/10.1016/j.molliq.2023.121259

Shirvani, M., Zhang, T., Gu, Y. & Hosseini-Sarvari, M. 2025. Sorghum grain as a bio-template: Emerging, cost-effective, and metal-free synthesis of C-doped g-C_3N_4 for photo-degradation of antibiotic, bisphenol A (BPA), and phenol under solar light irradiation. *Journal of Environmental Science and Pollution Research*, 32(4), pp.2036-2054. Available at: https://doi.org/10.1007/s11356-024-35868-1

Sobuś, N. & Czekaj, I. 2021. Comparison of synthetic and natural zeolite catalysts' behavior in the production of lactic acid and ethyl lactate from biomass-derived dihydroxyacetone. *Journal of Catalysts*, 11(8), p.1006. Available at: https://doi.org/10.3390/catal11081006

Song, S., Wu, G., Dai, W., Guan, N. & Li, L. 2016. Al-free Fe-beta as a robust catalyst for selective reduction of nitric oxide by ammonia. *Journal of Catalysis Science & Technology*, 6(23), pp.8325–8335. Available at: https://doi.org/10.1039/C6CY02124G

Sun, H., Li, J., Zhang, Y., Zhuang, L., Zhou, Z., Ren, Y., Xu, X., He, J. & Xue, Y. 2025. Treatment of high concentration phenol wastewater by low-frequency ultrasonic cavitation and long-term pilot scale study. *Journal of Chemosphere*, 370, p.143937. Available at: https://doi.org/10.1016/j.chemosphere.2024.143937

Sun, L., Zhang, X., Chen, L., Zhao, B., Yang, S. & Xie, X. 2016. Comparison of catalytic fast pyrolysis of biomass to aromatic hydrocarbons over ZSM-5 and Fe/ZSM-5

catalysts. *Journal of Analytical and Applied Pyrolysis*, 121, pp.342–346. Available at: https://doi.org/10.1016/j.jaap.2016.08.015

Taran, O.P., Zagoruiko, A.N., Yashnik, S.A., Ayusheev, A.B., Pestunov, A.V., Prosvirin, I.P., Prihodko, R.V., Goncharuk, V.V. & Parmon, V.N. 2018. Wet peroxide oxidation of phenol over carbon/zeolite catalysts: Kinetics and diffusion study in batch and flow reactors. *Journal of Environmental Chemical Engineering,* 6(2), pp.2551–2560. Available at: https://doi.org/10.1016/j.jece.2018.03.017

Thomsen, L. B. S., Anastasakis, K. & Biller, P. 2022. Wet oxidation of aqueous phase from hydrothermal liquefaction of sewage sludge. *Journal of Water research*, *209*, p.117863. Available at: https://doi.org/10.1016/j.watres.2021.117863

Tian, K., Pan, J., Liu, Y., Wang, P., Zhong, M., Dong, Y. & Wang, M. 2024. Fe-ZSM-5 zeolite catalyst for heterogeneous Fenton oxidation of 1, 4-dioxane: effect of Si/Al ratios and contributions of reactive oxygen species. *Journal of Environmental Science and Pollution Research* , *31* (13), pp.19738-19752. Available at: https://doi.org/10.1007/s11356-024-32287-0

Toloza-Blanco, L., Góra-Marek, K., Tarach, K. A., Sobalska, J., Martínez-Triguero, J., Plá-Hernandez, A. & Palomares, A. E. 2024. Catalytic oxidation of volatile organic compounds with Mn-zeolites. *Journal of Catalysis Today*, 432, p.114570. Available at: https://doi.org/10.1016/j.cattod.2024.114570

Treacy, M.M.J. & Higgins, J.B. 2007. *Collection of Simulated XRD Powder Patterns for Zeolites* (5th ed.). Amsterdam: Elsevier. Available at: https://doi.org/10.1016/B978-0-444-53067-7.X5470-7

Valkaj, K. M., Wittine, O., Margeta, K., Granato, T., Katović, A. & Zrnčević, S. 2011. Phenol oxidation with hydrogen peroxide using Cu/ZSM5 and Cu/Y5 catalysts. *Polish Journal of Chemical Technology*, *13*(3), pp.28-36. Available at: https://doi.org/10.2478/v10026-011-0033-6

Villegas, V. A. R., Ramirez, J. I. D. L., Perez-Sicairos, S., Yocupicio-Gaxiola, R. I., González-Torres, V. & Petranovskii, V. 2024. Catalyst for lactose hydrolysis based on zeolite Y modified with Fe species by ultrasound treatment. *Journal of Environmental Advances*, *15*, p.100475. Available at: https://doi.org/10.1016/j.envadv.2023.100475

Wang, H., Xu, R., Jin, Y. & Zhang, R. 2019. Zeolite structure effects on Cu active center, SCR performance and stability of Cu-zeolite catalysts. *Journal of Catalysis Today*, 327, pp.295-307. Available at: https://doi.org/10.1016/j.cattod.2018.04.035

Wu, Y., Zhang, H. & Yan. Y. 2020. Effect of copper ion-exchange on catalytic wet peroxide oxidation of phenol over ZSM-5 membrane. *Journal of Environmental Management*, 270, p.110907. Available at: https://doi.org/10.1016/j.jenvman.2020.110907

Xie, J., Zhuang, W., Yan, N., Du, Y., Xi, S., Zhang, W., Tang, J., Zhou, Y. & Wang, J. 2017. Directly synthesized V-containing BEA zeolite: Acid-oxidation bifunctional catalyst enhancing C-alkylation selectivity in liquid-phase methylation

of phenol. *Chemical engineering journal*, 328, pp.1031-1042. Available at: https://doi.org/10.1016/j.cej.2017.07.100

Zang, J., Yu, H., Liu, G., Hong, M., Liu, J. & Chen, T. 2023. Research progress on modifications of zeolite Y for improved catalytic properties. *Journal of Inorganics*, 11(1), p.22. Available at: https://doi.org/10.3390/inorganics11010022

Zhang, J., Shao, S., Guo, Q., Duan, X., Liu, Y. & Jiao, W. 2025. Co-removal of phenol and Cr (VI) by high gravity coupled heterogeneous catalytic ozonation-adsorption. *Journal of Separation and Purification Technology*, 358(Part A), p.130297. Available at: https://doi.org/10.1016/j.chemosphere.2024.143937

Zhou, X., Wang, M., Yan, D., Li, Q. & Chen, H. 2019. Synthesis and performance of high efficient diesel oxidation catalyst based on active metal species-modified porous zeolite BEA. *Journal of Catalysis*, 379, 138-146. Available at: https://doi.org/10.1016/j.jcat.2019.09.029

Компаративна студија два различита зеолита, BEA и ZSM-5, модификована бакром и гвожђем током оксидације фенола водоник-пероксидом

Фатиха Талхауи[а], **аутор за преписку**, *Фатиха* Хамиди[а], *Франсиско* Медина[б]

[а] Универзитет наука и технологије „Мухамед Будијаф", Хемијски факултет, Лабораторија функционалних и наноструктурираних екоматеријала, Оран, Алжир.

[б] Катедра за хемијско инжењерство, Универзитет „Ровира и Виргили", Авингуда делс Паисос Каталанс, 26, 43007, Тарагона, Шпанија.

ОБЛАСТ: материјали, хемијска технологија
ВРСТА ЧЛАНКА: оригинални научни рад

Резиме:

Увод/циљ: Загађење воде органским једињењима као што је фенол представља значајан еколошки ризик. Циљ овог истраживања био је да се упореди каталитичка ефикасност зеолита ZSM-5 и BEA, модификованих гвожђем (Fe) и бакром (Cu), у мокрој оксидацији фенола коришћењем водоник-пероксида (H_2O_2).

Метод: Зеолити BEA и ZSM-5 синтетисани су хидротермалним методама, а затим подвргнути јонској размени ради уношења Cu^{2+} и Fe^{2+}. Катализатори су окарактерисани техникама XRD, FTIR, SEM и XPS. Оксидација фенола извођена је на 80°C у воденој средини, са моларним односом H_2O_2/фенол између 10:1 и 15:1. Реакциони производи анализирани су методом HPLC.

Резултати: Кристална структура зеолита очувана је након јонске размене. Метали су били равномерно распоређени на површини. Катализатори Fe-BEA и Fe-ZSM-5 показали су највећу активност (до 99% конверзије), затим Cu-BEA (88%) и Cu-ZSM-5 (68%). Чисти зеолити показали су ниску активност (<10%). Оптималан однос

H_2O_2/фенол био је 14:1. Fe-BEA се показао као најефикаснији катализатор, комбинујући високу активност и бољу дифузију у порама.
Закључак: Зеолити модификовани гвожђем, посебно Fe-BEA, представљају веома ефикасне катализаторе за оксидацију фенола у воденој средини, надмашујући како узорке модификоване бакром, тако и чисте зеолите. Порозност структуре и природа метала кључни су фактори који одређују каталитичке перформансе.

Кључне речи: ZSM-5, BEA, водоник-пероксид, оксидација фенола, хетерогена катализа

Paper received on: 28.03.2025.
Manuscript corrections submitted on:03.04.2025.
Paper accepted for publishing on: 04.05.2025.